Materials and Manufacturing Processes, 22: 170–174, 2007

ISSN: 1042-6914 print/1532-2475 online
DOI: 10.1080/10426910601062206

Taylor & Francis
Taylor & Francis Group

Creep of Al Underlayer Determined by Channel Cracking of Topical Si_3N_4 Film

Seyed M. Allameh[1], Zhigang Suo[2], and Wole Soboyejo[1]

[1]*Department of Mechanical and Aerospace Engineering, Princeton University, USA*
[2]*Division of Engineering and Applied Sciences, Harvard University, USA*

This paper presents the results of channel cracking experiments performed on a multilayered structure. Room temperature creep behavior of a metallic underlayer was studied by using a newly developed channel cracking method. By the analysis of a channel crack propagating under tensile load in an elastic Si_3N_4 topical layer, the creep properties of an aluminum underlayer were determined. The experimental results were compared with the results of room temperature creep studies performed on commercial Al and Al–Mg micro-wires. As expected, the viscosity of pure Al underlayer is less than that of these materials. It is about 50% of the viscosity attributable to the primary creep region of commercial Al micro-wires. Compared to the viscosity of a harder alloy, the viscosity of the pure Al underlayer is about 20% of that attributable to the primary creep region of Al–Mg micro-wires. The growing cracks are observed to terminate at surface flaws that relieve their stress fields.

Keywords Channel cracking; Crack growth; Creep; Multilayer structure; SiN; Thin films.

Introduction

The reliability of microelectronics and microdevices used in various applications including computers, automotive industry and biomedical fields greatly depend on the mechanical properties of the materials [1–3]. Since mechanical behavior of small structures used in microelectronic and microelectromechanical devices (MEMS) differ from those of bulk materials, it is necessary to conduct micro-mechanical tests on these materials in their final geometries [4–7]. Room-temperature creep of metallic layers in microelectronics and metallic components in MEMS can lead to unexpected failure of these devices [8, 9].

Channel cracking [9–15] has been developed to study and compute [10, 16] the steady state energy release rate of channeling cracks in thin films. The application of this method is important in the prediction of the fracture behavior of multilayered structures that are under residual stress developed during the fabrication process. In the presence of a sharp corner or a microcrack, the stress field intensifies at the interface between dissimilar materials.

Residual stress is not the only component that affects the failure of structures. Other parameters such as thickness of the layers will play an important role in the failure process. The successful application of multilayered structure relies on designs that optimize processing variables. These include: residual stresses, the thickness of the individual layers, as well as the type of the materials used in each layer.

In multilayered structures consisting of dissimilar materials, cracking of one layer may lead to the plastic deformation of another. Consider crack extension in an elastic Si_3N_4 layer deposited on an Al thin film, which, in turn, is deposited on Si. Crack propagation in the topical Si_3N_4 layer can reach a steady state, which is dictated by two parameters: the rate of decohesion at the crack tip and the rate of creep of the Al layer.

Shear lag models have been used to study cracking of brittle films deposited on viscous [9, 11, 14]. Liang et al. [11] developed a shear lag model that approximates the fracture process in an elastic film blanketing a metal underlayer. The creep properties of the underlayer and the fracture toughness of the topical inelastic layer are inter-related such that if one is known the other one can be calculated. Ma et al. [12, 13] studied channel cracking in brittle Si_3N_4 films deposited on Al [12] and on Si [13] substrates. They reported two different values for the fracture toughness of Si_3N_4, as will be discussed later.

Under bending loads, both Al and Si_3N_4 layers are under tension. At high stress levels, beyond the yield point of Al, the Si_3N_4 layer experiences elastic strains while the Al underlayer undergoes plastic deformation. The system remains in equilibrium if no cracking occurs. However, once a crack is initiated in the Si_3N_4 layer, the stress intensity in the vicinity of the crack tip causes further deformation of the Al underlayer. This additional strain accumulated in the Al film can be attributed to the presence of excess stress at the crack tip.

In this paper, the approach of Liang et al. [11, 15, 16] has been adopted to study the room-temperature time-dependent deformation of an Al layer undergoing creep concurrent with the propagation of crack in its Si_3N_4 overlayer. The information obtained here will be complementary to the mechanical properties of bulk Al and Al alloys [17–19] on micron scale. These include room temperature creep properties [20, 21] obtained for thin aluminum micro-wires.

Theory

This section presents an overview of the underlying theory that was used to extract the creep viscosity. For brevity,

Received April 2, 2004; Accepted April 8, 2005
Address correspondence to Seyed M. Allameh, Department of Physics and Geology, Northern Kentucky University, USA; E-mail: allamehs1@nku.edu

the theory is only summarized here. More complete descriptions of the underlying theoretical framework can be found in papers by Liang et al. [11, 15, 16].

For the current problem of multilayered coatings consisting of 2 mm Al films on a 4 mm thick Si_3N_4 layer deposited on a Si substrate, Liang et al. [11, 15, 16] have modeled the effects of creep on the Al underlayer on the driving force for channel crack growth in the Si_3N_4 layer. Since the underlying Al layer can creep at room temperature [20–22] the total strain in the Al foil (e.g. plastic + elastic) should be equal to the elastic strain of Si_3N_4 at the crack tip.

$$\varepsilon_e^{\mathrm{Al}} + \varepsilon_p^{\mathrm{Al}} = \varepsilon_e^{\mathrm{Si_3N_4}} \tag{1}$$

However, the far field stresses are elastic in both Al and Si_3N_4 layers. The stress in the Si substrate can be calculated from the load applied to the specimen:

$$\sigma_{\mathrm{Si}} = -\frac{3PLy}{bh_{\mathrm{Si}}^3} \tag{2}$$

where P is the applied load, y is distance from the neutral axis of the wafer, L is the support span, b is the width of the sample and h_{Si} is the thickness of the wafer. The stress in the Si_3N_4 film can be calculated from the superposition of the residual stress as follows:

$$\sigma_{\mathrm{Si_3N_4}} = \sigma_{res} + \sigma_{\mathrm{Si}} \frac{1-\nu_s^2}{1-\nu_f^2} \quad \frac{E_{\mathrm{Si_3N_4}}}{E_{\mathrm{Si}}} \tag{3}$$

The steady state velocity of crack tip, V_{ss}^{∞}, can be related to the thickness of Si_3N_4 film, h, thickness of Al, H, Young's Modulus of the Si_3N_4 film, $E_{\mathrm{Si_3N_4}}$, stress magnitude in the Si_3N_4 film, $\sigma_{\mathrm{Si_3N_4}}$, viscosity of the underlying Al layer, η, and the fracture toughness of the Si_3N_4film, K_c through a dimensionless parameter χ as following:

$$V_{ss}^{\infty} = \chi \frac{HhE_{\mathrm{Si_3N_4}}\sigma_{\mathrm{Si_3N_4}}^2}{\eta K_c^2} \tag{4}$$

Equation 3 can be solved either for the η or K_c. If one is known the other one can be calulated. Rearranging the terms in Eq. 4, the viscosity of Al can be obtained from

$$\eta = \frac{\chi HhE\sigma_0^2}{K_c^2 V_{ss}^{\infty}} \tag{5}$$

Finally the fracture toughness of a brittle film on an elastic substrate can be calculated from the following [12, 13]:

$$G_c = \alpha \frac{(1-\nu^2)\,\sigma_f^2 h_f}{E_f} \tag{6}$$

Here α is a dimensionless function that depends on the elastic mismatch between the film and the substrate. It also includes any plasticity involved in the process.

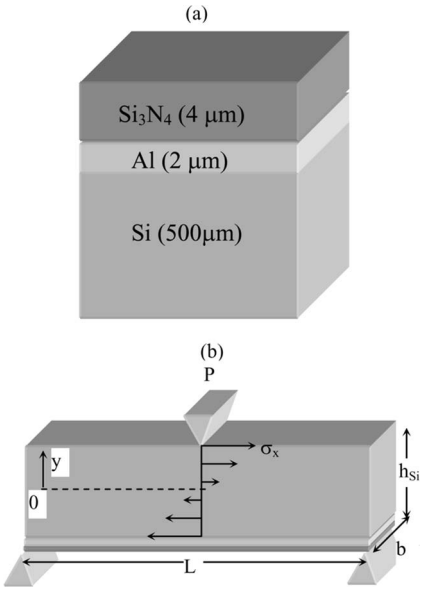

FIGURE 1.—(a) Schematic of order of films on Si substrate, (b) Loading of the sample in three point bend configuration with the films being placed under tensile loading.

An approximation of this parameter, derived from shear lag models is presented by Hu and Evans [23] as follows:

$$\alpha = \frac{\sigma_f}{\sqrt{3}\sigma_y} + \alpha_{el} \tag{7}$$

There are two components in the above relationship: plastic and elastic. While the plastic component is a function of the yield stress of the metal underlayer, σ_y, and the film stress of the Si_3N_4 layer, σ_f, the elastic component is only a weak function of the elastic mismatch between the film and the substrate.

EXPERIMENTAL PROCEDURE

The samples that were used in this study were supplied by Dr. Qing Ma of Intel Corporation, Santa Clara, Calif. The multilayered samples consisted of Si substrates that were coated with a 2 μm Al film on which a 4 μm thick Si_3N_4 was grown (Fig. 1a). The topical Si_3N_4 film was examined for residual stress, which was determined to be compressive in nature, with a magnitude of 97.9 MPa. A test sample was cut from the substrate with dimensions of ~10 mm × ~32 mm. The sample was subsequently loaded in the bending apparatus, as shown in Fig. 1(b) and Fig. 2.

The loading device (Fig. 2) consisted of a thumb wheel screw attached to the load frame mounted in series with an Entran™ micro-load cell that measured the load during the test. The load was applied by imposing strain at the center of the sample using a a flexure blade connected to the load cell. The surface of the sample was initially scratched with a diamond pen to create microcracks at the edge of the

™Entran is trade mark for Entran Devices Inc., Fairfield NJ 07004.

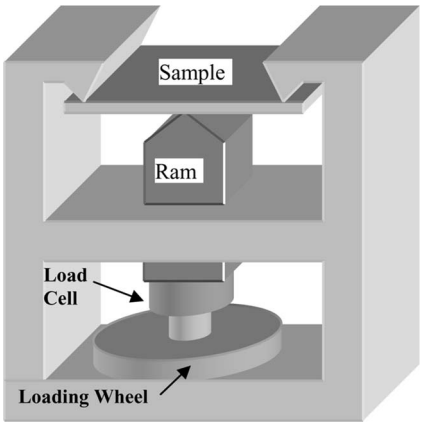

FIGURE 2.—Schematic of loading device for channel cracking of Si_3N_4 on Al on Si.

sample. A monoscope equipped with a video camera, and a tape recorder was used to capture the images during crack growth. The loci of the crack tip were determined from the consecutive images and were plotted against time. These plots were then used to calculate crack tip velocity.

RESULTS AND DISCUSSION

Crack Growth

The orientation of the channel crack and its propagation direction relative to the edge of the sample is shown in Fig. 3. The loci of the crack-tip (recorded versus time) are presented in Fig. 4. A typical picture of the cracks is shown in Fig. 5. While a crack has swept the area on the right hand side of the image, a second crack has stopped in the presence of a surface flaw that has apparently relaxed the stress field in the vicinity of the crack tip. A new crack has grown in a nearby location in lieu of continuation of the stopped crack.

For the crack growth rate of 2.67×10^{-6} m/s obtained in the current study, Eq. 5 and the material property data presented in Table 1 were used to estimate the viscosity of Al film. This gives a viscosity of 9.6×10^{16} Pa.s as shown in Table 1. The values of χ, ν, and E for the films and the substrates are taken from Liang et al. [11, 15, 16] and Ma et al. [12, 13]. The calculated value is based on the

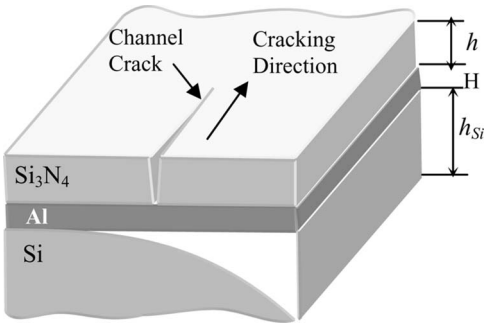

FIGURE 3.—Channel cracking of the topical Si_3N_4 layer deposited on Al underlayer.

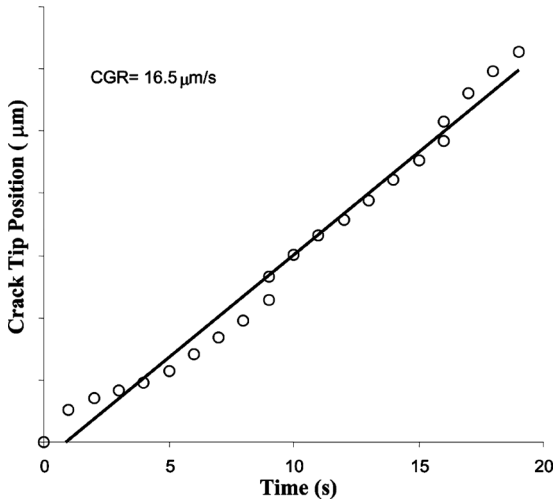

FIGURE 4.—Crack growth rate of Si_3N_4 on Al on Si.

fracture toughness values obtained by Ma et al. [13] from channel cracking experiments performed on Si_3N_4 films grown on Si.

FRACTURE TOUGHNESS

Ma et al. [12, 13] have reported two values for the fracture toughness of Si_3N_4 based on the nature of substrates. A fracture toughness of 4.9 J/m^2 was reported [13] for Si_3N_4 deposited on Si. Using a metal underlayer, Ma et al. [12] obtained a different fracture toughness value of 8.7 J/m^2 for Si_3N_4 deposited on Al film. This aluminum film was deposited on SiO_2 grown on Si.

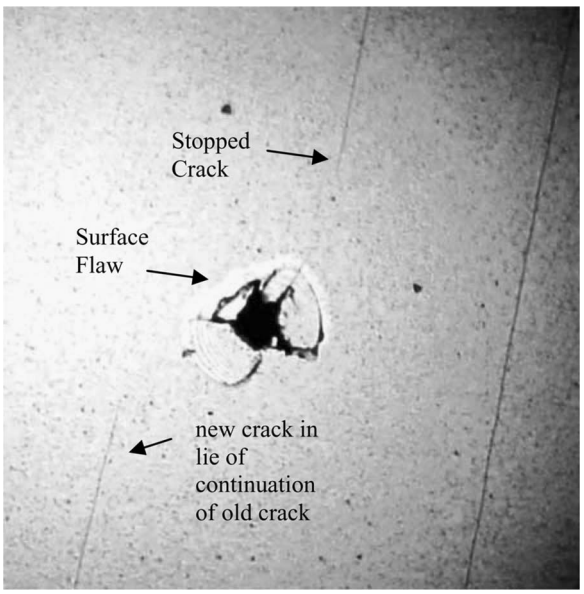

FIGURE 5.—Interaction of a growing crack with a surface flaw. The crack has terminated and a new crack has initiated. Relaxation of stress field in the vicinity of the flaw has stopped the crack.

TABLE 1.—Calculation of various parameters leading to the viscosity of Al. Values for E_{Si}, E_{SiN}, $K_{c,QM}$, ν_{Si} ν_{SiN}, χ, and α_{el} and $\sigma_{y,Al}$ are from Refs. [12, 13, 15, 16].

Calculation of stress		Calculation of viscosity		Calculation of G	
$\sigma_{residual}$	97.90 MPa	E_{Si}	169E + 05 MPa	$\sigma_{maxi,SiN}$	440 Mpa
b	9.83 mm	H_{Al}	2.00E − 06 m	ν_{Si}	0.25
L	30.00 mm	h_{SiN}	4.00E − 06 m	ν_{SiN}	0.25
P	2.45 kg	E_{SiN}	1.95E + 05 MPa	σ_{SiN}	381 MPa
L	30.00 mm	V_{ss}	1.65E − 05 m/s	σ_{total}	$\sigma_{max} + \sigma_{residual}$
Y_{max}	0.25 mm	χ	0.613	$\sigma_{total,SiN=\sigma_f}$	479 MPa
h_s	0.50 mm	$K_{c,QM}$	$9.47E - 01$ MPam$^{1/2}$	$\sigma_{y,Al}$	75 MPa
$\sigma_{max,Si}$	44.8 kg/mm^2	σ_0	4.79E + 02 MPa	α	5.68
$\sigma_{max,Si}$	440 MPa	η	$(\chi HhE\sigma_0^2)/(V_{ss}{}^* K_{c,QM}^2)$	$G_{c,apparent}$	25.06 J/m^2
		η	1.48E + 16 Pa.s	$K_{c,apparent}$	2.21 MPam$^{1/2}$

The difference between the two values of fracture toughness that Ma et al. obtained for two Si_3N_4 film on two different substrates (e.g. $8.7 - 4.9 = 3.8$ J/m^2) can be attributed to the energy expended for the viscous flow of Al underlayer. Apparently Eq. 6 is more appropriate for brittle films on elastic substrates. Using Eqs. 6 and 7 and ignoring the effect of Al creep, a value of 25 J/m^2 is obtained for the apparent fracture toughness of Si_3N_4 deposited on Al (Table 1). This apparent value cannot be used for the fracture toughness of Si_3N_4. In fact, the true fracture toughness of topical Si_3N_4 can be obtained if the viscosity of Al is known. Since Ma et al. [13], (4.9 J/m^2) have independently examined the fracture toughness of Si_3N_4 deposited on Si, their number could be used to calculate the viscosity of the Al underlayer. Equations 2–5 are used for this purpose.

Room-Temperature Creep in Al and Al Alloys

The importance of the room temperature creep of Al is not only important for microelectronics and microdevices, but also in bulk materials. Al alloys have been adopted in drift chambers to minimize multiple scattering. The tension of these wires mitigates with room temperature creep [20].

Like many low melting point meals, Al [20, 24] and Al alloys [21] tend to creep at room temperature more than some other materials [19, 22]. This creep occurs not only in bulk Al wires [20, 21] but also in thin films used in microelectronics [11, 12, 15]. Recovery and recrystallization of metals and alloys usually occur at a temperature that falls within 0.3 to 0.5 of their melting point T_m) on an absolute temperature scale. Creep of Al is possible at room temperature where $T/T_m = 0.32$ (within the 0.3–0.5 range).

The results of room temperature viscosity of Al obtained here can be compared with the room temperature creep properties of Al alloys including Al micro-wires reported by Lu and McDonald [20]. Under stress levels of 200 MPa, these authors obtained strain rates of 1.7×10^{-10} s^{-1} to 1.7×10^{-9} s^{-1} for the initial and steady state stages of creep respectively. Higher creep rates were reported for Al–Mg alloys tested by Bencivenni et al. [21]. Under stress levels of 172 MPa, they reported initial creep rates equivalent to about 5.5×10^{-10} s^{-1} and a steady state creep rate of about 1.7×10^{-10} s^{-1} The shear strain rate, $\dot{\gamma}$, attributable to these creep rates can be converted into an apparent viscosity, η, by:

$$\tau = \eta\dot{\gamma} \tag{8}$$

where τ is shear stress associated with creep process. The creep results mentioned above can be converted into apparent viscosities, assuming that deformation occurs by shear on the planes of maximum resolved shear stress. The apparent viscosities associated with the creep rates reported by Lu and McDonald [20] will be 2.9×10^{16} Pa.s for the initial creep stage and 2.9×10^{17} Pa.s for the steady state creep stage. The corresponding viscosities associated with the creep of Al–Mg alloy, reported by Bencivenni et al. [21] will be 8.5×10^{16} Pa.s for the initial stage and 2.5×10^{17} Pa.s for the steady state creep stage.

The value of viscosity of pure Al obtained in this study (1.48×10^{16} Pa.s) is nearly one half of the viscosity attributable to the initial stage of creep of commercial Al micro-wires reported by Lu and McDonald [20]. A higher creep resistance is expected for these wires due to strengthening effects of alloying elements. In comparison with a harder Al alloy, our calculated viscosity is 20% of the value attributable to the initial stage of Al–Mg alloy [21]. This suggests that creep of pure Al film is much faster than that of 5056 Al-Mag alloy wire at room temperature [21]. This alloy contains 4.5−5.6% Mg, 0.10% Cu, 0.30% Si, 0.40% Fe, 0.05−0.20% Mn, 0.1% Zn and 0.05−0.20% Ti [25]. The higher viscosities of the Al–Mg alloy can be attributed to the presence of alloying elements that promote creep strengthening [26, 27].

The presence of alloying elements in the Al alloys can increase the energy release rate associated with the cracking of the Si_3N_4 film deposited on the Al alloy layer. The increase in the energy release rate will be through an increase in the viscosity of the Al underlayer. The increase in the creep resistance of Al–Mg alloy has been related to the effects of Mg solute atoms and also to the presence of particles in the grain boundaries [27]. Usually 3% Mg is enough to promote solute drag creep in Al–Mg alloys [17, 22]. Magnesium solutes are believed to interact with the grain boundary dislocations during creep of Al–Mg [27]. This suggests that alloyed Al films may be used to improve the creep resistance and the resistance to channel cracking in the type of multilayered films examined in this study.

Summary and concluding remarks

Based on the channel cracking experiments performed on multilayers of Si_3N_4/Al/Si tested under a stress level of 479 MPa (in Si_3N_4 film) the following conclusions are reached:

1) The apparent viscosity of Al underlayer obtained in this study is 1.48×10^{16} Pa.s. This apparent viscosity is nearly 1/2 of viscosity attributable to the primary creep of Al micro-wires. Compared with the harder Al–Mg alloy, the viscosity of pure Al underlayer is about 1/5 of that attributable to the primary creep region of Al–Mg.
2) Growing cracks were observed to terminate in the vicinity of surface flaws where stress fields are relaxed. The apparent energy release rate for the growing cracks was $\sim$25 J/m^2 which includes the energy required for the creep of Al underlayer.
3) The current results suggest that multilayered structures with Al underlayer can be improved by alloying to improve the room-temperature creep resistance.

Acknowledgments

This research was supported by the Division of Materials Research of The National Science Foundation (NSF) (Grant No.). The authors are grateful to Dr. Carmen Huber, Program Manager of NSF, for her encouragement and support.

References

1. Brown, S.B.; Jansen, E. Reliability and long term stability of MEMS. *Presented in LEOS Summer Topical Meeting*; IEEE.: Piscataway, NJ; 1996.
2. Evans, J.W.; Evans, J.Y. Reliability assessment for development of microtechnologies. Microsystem Technologies **1997**, *3* (4), 145–154.
3. Togawa, T. *Biomedical Transducers and Instruments*; CRC Press; 1997.
4. Ding, J.N.; Meng, Y.G.; Wen, S.Z. Size effect on the mechanical properties and reliability analysis of microfabricated polysilicon thin films. Presented in Annual Proceedings – Reliability Physics (Symposium) 2001; 106–111.
5. Kahn, H.; Heuer, A.H.; Ballarini, R. On-chip testing of mechanical properties of MEMS devices. MRS Bulletin **2001**, *26* (4), 300–301.
6. Sharpe, Jr., W.N.; Jackson, K.M.; Hemker, K.J.; Xie, Z. Effect of specimen size on Young's modulus and fracture strength of polysilicon. Journal of Microelectromechanical Systems **2001**, *10* (3), 317–326.
7. Baker, S.P.; Vinci, R.P.; Arias, T. Elastic and anelastic behavior of materials in small dimensions. MRS Bulletin **2002**, *27* (1), 26–29.
8. Vickers-Kirby, D.J.; Kubena, R.L.; Stratton, F.P.; Joyce, R.J.; Chang, D.T.; Kim, J. Anelastic creep phenomena in thin metal plated cantilevers for MEMS. Materials Research Society Symposium – Proceedings **2001**, *657*, EE251–EE256.
9. Huang, R.; Prevost, J.H.; Suo, Z. Loss of constraint on fracture in thin film structures due to creep. Acta Materialia **2002**, *50* (16), 4137–4148.
10. Huang, R.; Prevost, J.H.; Huang, Z.Y.; Suo, Z. Channel-cracking of thin films with the extended finite element method. Engineering Fracture Mechanics **2003**, *70* (18), 2513–2526.
11. Liang, J.; Huang, R.; Prévost, J.H.; Suo, Z. Thin film cracking modulated by underlayer creep. Experimental Mechanics **2003**, *43* (3), 269–279.
12. Ma, Q.; Tran, Q.; Sun, B.; El-Mansy, S.; Sun, J.; Fujimoto, H. Measurement of toughness for SiN films on silicon using channel cracking technique. *Presented in Materials Reliability in Microelectronics IX. Symposium*. Mater. Res. Soc.: San Francisco, CA, USA, 1999; 285–290.
13. Ma, Q.; Xie, J.; Chao, S.; El-Mansy, S.; McFadden, R.; Fujimoto, H. Channel cracking technique for toughness measurement of brittle dielectric thin films on silicon substrates. Materials Research Society Symposium – Proceedings **1998**, *516*, 331–336.
14. Lehner, F.K.; Li, V.C.; Rice, J.R. Stress diffusion along rupturing plate boundaries. Journal of Geophysical Research **1981**, *86* (B7), 6155–6169.
15. Liang, J.; Zhang, Z.; Prévost, J.H.; Suo, Z. Time-dependent crack behavior in an integrated structure. International Journal of Fracture, **2004**, *125* (2), 335–348.
16. Liang, J.; Huang, R.; Prévost, J.H.; Suo, Z. Evolving crack patterns in thin films with the extended finite element method. International Journal of Solids and Structures **2003**, *40* (10), 2343–2354.
17. Taleff, E.M.; Nevland, P.J.; Krajewski, P.E. Tensile ductility of several commercial aluminum alloys at elevated temperatures. Metallurgical and Materials Transactions A (Physical Metallurgy and Materials Science) **2001**, *32A* (5), 1119–1130.
18. Vinci, R.P.; Bravman, J.C. Mechanical testing of thin films. Presented in TRANSDUCERS '91. 1991 International Conference on Solid-State Sensors and Actuators. Digest of Technical Papers (Cat. No. 91CH2817-5). San Francisco, CA, IEEE, 1991; 943–948.
19. Vinci, R.P.; Cornella, G.; Bravman, J.C. Anelastic contributions to the behavior of freestanding Al thin films. Presented in AIP Conference Proceedings Stuttgart, Germany, AIP, 1999; 240–248.
20. Lu, C.; McDonald, K.T. *The Effect of Annealing on Creep of Aluminum Wire*; Princeton University: Princeton; 1997, 1–14.
21. Bencivenni, G.; Bucci, L.; Finocchiaro, G.; Forti, C. *Creep Measurement on Aluminum-5056 Wires*; KLOE: Frascati, Italy, 1998; 1–13.
22. Kubota, Y.; Nelson, J.K.; Perticone, D.; Poling, R.; Schrenk, S.; Alam, M.S. The CLEO II detector, nuclear instruments & methods in physics research, section A (Accelerators, Spectrometers, Detectors and Associated Equipment) **1992**, *A320* (1–2), 66–113.
23. Hu, M.S.; Evans, A.G. The cracking and decohesion of thin films on ductile substrates. Acta Metallurgica **1989**, *37* (3), 917–925.
24. El-Deiry, P.A.; Vinci, R.P. Strain rate dependent behavior of pure aluminum and copper micro-wires. Materials Research Society Symposium – Proceedings **2002**, *695*, 159–164.
25. Standard Specification, Wrought Aluminum Alloys: Composition and The Characteristics. Elemans Corporation, Seoul, Korea, http://www.elemans.com/2/specifications.html.
26. Ozturk, K.; Zhong, Y.; Luo, A.A.; Liu, Z.-K. Creep resistant Mg–Al–Ca alloys: computational thermodynamics and experimental investigation. JOM **2003**, *55* (11), 40–44.
27. Hayes, R.W.; Tellkamp, V.; Lavernia, E.J. Creep behavior of a cryomilled ultrafine-grained Al-4% Mg alloy. Journal of Materials Research **2000**, *15* (10), 2215–2222.